Appl. Phys. B 71, 277–284 (2000) / Digital Object Identifier (DOI) 10.1007/s003400000346

Applied Physics B
Lasers
and Optics

Optimal control of one- and two-photon transitions with shaped femtosecond pulses and feedback

T. Hornung, R. Meier, D. Zeidler, K.-L. Kompa, D. Proch, M. Motzkus*

Max-Planck-Institut für Quantenoptik, 85740 Garching, Germany

Received: 3 November 1999/Published online: 5 July 2000 –

Abstract. This paper reports two pump–probe experiments in sodium where dynamically tailored ultrashort pulses from a Ti:Sapphire-pumped optical parametric amplifier were employed. The first study focuses on the one-photon Na($3s \rightarrow 3p$) transition to derive sensitive criteria which judge the performance of a frequency-domain pulse shaper using a spatial light modulator. On the basis of the interpretation, follow-up experiments are suggested to test their cogency. The second experiment uses coherent quantum control by placing an appropriate phase distribution on the incident beam to enhance or cancel the transition probability in the nonresonant two-photon process Na($3s \rightarrow\rightarrow 5s$). Ignorant of the "ideal" phase function, an evolutionary algorithm which uses a feedback derived from the experiment performs the optimization and produces the desired bright or dark pulses within a few minutes. Attention is given to the role of resonant $3s \rightarrow 3p$ transitions excited by the spectral wings of the pump pulse. Different parametrizations of the phase distribution have been examined. Two of these produced solutions which had not previously been predicted by theory still meet the objective of the experiment. The study represents the first successful application of a feedback-organized self-learning algorithm to the design of dark pulses.

PACS: 32.80.Qk; 42.50.Gy; 42.65.Re

The capability to tailor ultrashort femtosecond pulses and thus synthesize almost arbitrary waveforms, which has been a subject of intensive and successful work in the recent past, has paved the way towards experiments which aim at a control of quantum-mechanical phenomena [1–3]. The conceptional scheme which has been proposed to this end, and which has been termed *coherent* – or *optimal control*, tends to maneuver an atomic or molecular system towards a desired target state through a suitable interaction with light [4–7]. This objective can be achieved through quantum interference between distinct competing routes leading to this final state. The occurrence of either constructive or destructive interference depends on the spectral phase and amplitude distribution of the pump beam. Optimal control of quantum interactions thus relies on the effective manipulation of the coherence properties of the optical field.

The most effective techniques to shape ultrashort optical pulses into desired waveforms rest upon filtering of the spectrally dispersed original pulse in the Fourier plane. The first demonstration of frequency-domain pulse shaping in the femtosecond (fs) regime by using a spatially patterned mask to place an appropriate phase on the frequency spectrum has been reported by Weiner et al. [8]. Weiner's group, a few years later, was also the first to demonstrate the production of almost arbitrarily shaped fs pulses via programmable dynamic phase-only filtering [9–11]. Expanded flexibility is afforded by a shaper design which allows independent dynamic control of phase and amplitude, as introduced by Wefers and Nelson [12, 13]. A different approach to tailor fs pulses in phase and amplitude is based on acousto-optical modulation (AOM) and has been explored extensively by Warren and co-workers [14]. Other techniques to shape ultrashort pulses have been employed as well [15, 16].

The synthesis of waveforms which drive a quantum-mechanical system towards a selected terminal state requires complete knowledge of the Hamiltonian. With the exception of di- and sometimes tri-atomic molecules this operator is generally unknown, which complicates or even precludes the direct calculation of the spectral filter creating the desired output pulse. These restraints can be bypassed by using an adaptive approach [7, 11, 17, 18] in the sense that an interactive dialogue is established between the experiment and a self-learning algorithm which controls the phase mask. Several successful implementations of this principle have been reported since then [1–3, 19–21].

The task of the algorithm which processes input from the experiment is to optimize a merit function which indicates the adequacy of the manipulated pulses to achieve a preset goal. If intelligently parametrized, the procedure will eventually zoom into an optimum which, however, need not necessarily be the global extremum. An interpretation as to why control is achieved is not straightforward.

*Corresponding author. (E-mail: mcm@mpq.mpg.de)

This paper reports two pump–probe experiments performed on sodium. Data from the one-photon Na($3s \rightarrow 3p$) study directly reflect the performance and fidelity of the pulse shaper. Based on the results we may judge on principal limitations of the shaping process and quantify its sensitivity to a variation of the influencable parameters. The data also afford a critical test of the validity of analytical descriptions of coherently controlled one-photon excitation [22]. The nonresonant two-photon process Na($3s \rightarrow\rightarrow 5s$) represents an example of effectively controlled energy deposition in a two-level system by tailoring the spectral phase of the pump pulse, using an additionally implemented feedback scheme. Three different parametrizations of the phase have been tested and solutions of the "best" phase functions have been found which had not previously been predicted by theory. In all cases the global minimum of the cost function is asymptotically approached within a short time. This is, at least to the best of our knowledge, the first demonstration of *dark pulses* that have been designed by a genetic algorithm which only processes information received from the experiment, i.e. free from any initial constraints dictated by theoretical deliberations.

1 Experimental setup

The femtosecond pulse source for both experiments was a commercial Ti:sapphire laser system (CPA-1000, Clark MXR Inc.) which supplied 1 mJ/100 fs/800 nm pulses at a repetition rate of 1 kHz. Frequency conversion to the wavelength interval between 580 nm and 700 nm in an optical parametric amplifier (IR-OPA, Clark) yielded pulse energies around 5 μJ. The programmable pulse-shaping apparatus is a symmetric 4-f arrangement [8, 23] composed of one pair each of reflective gratings (1800 lines/mm) and cylindrical lenses ($f = 150$ mm). Its active element – a liquid-crystal (LC) mask – is installed in the common focal plane of both lenses. Meticulous alignment must ensure zero net temporal dispersion. This is achieved once the shapes of input and output pulses match as long as the LC mask is turned off. The technique of frequency-resolved optical gating (FROG) [24] served to characterize the generated pulses.

Sodium was evaporated in a heat pipe oven [25] pressurized with 10 mbar of argon as a buffer gas. The temperature was set sufficiently low (520 K) to eliminate pulse-propagation effects [26, 27]. Details of the excitation and detection schemes will be supplied in the context of the respective experiments.

2 Dynamic pulse shaping by spatial light modulation

The core of the pulse-shaper unit is an externally addressable pair of one-dimensional liquid-crystal arrays sandwiched between two parallel (horizontal) polarizers (SLM-256, Cambridge Research & Instrumentation). Voltage to each individual strip of this structure is supplied through a matching pattern of indium–tin oxide (ITO) electrodes bonded to the surfaces of the nematic-crystal arrays. This spatial light modulator (SLM) permits independent control of phase and amplitude for each of its $n = 1 \ldots 128$ pixels [13, 28].

In the time domain the modulation of the frequency spectrum results in a pulse $e_{\text{out}}(t)$ which may be expressed as a summed sequence of evenly spaced input pulses $e_{\text{in}}(t)$, each characterized by an amplitude a_n and a phase Φ_n [23]:

$$e_{\text{out}}(t) = \sum_n a_n \exp(i\Phi_n) e_{\text{in}}(t + n\tau) \,. \tag{1}$$

To perform efficient shaping the bandwidth of the incident pulse must fit on the active area of the mask. Observing this requirement, the parameter τ, which subsumes the dispersion property of the reflective grating and the dimensional parameters of the mask (interpixel distance, total number of pixels) is connected to the incident pulse width, t_{pulse}, by $\tau \approx 0.5 \times t_{\text{pulse}}$ [23]. The summation must be carried over the total number of pixels (128) and hence covers a maximum shaping window of $128 \times \tau$. The amplitude and phase coefficients, a_n and Φ_n, are related to the transmission and retardance values placed on the modulator via a discrete complex Fourier transformation. Since this is a fast procedure, any desired pulse as expressed by (1) can be synthesized within less than one second [29]. The concurrent manipulation of phase and amplitude incurs a loss of pulse energy which may be unacceptable. This drawback can be remedied to some extent by phase-only filtering [30–32] which leaves the power spectrum and the energy of the shaped pulse intact. The approach is, however, disadvantageous since it limits the potential of modulation.

The optimization algorithm which is in control of the pulse-shaping device is supposed to interpret a signal from the experiment and develop a strategy which eventually pinpoints the global minimum of a multidimensional cost function. A coarse classification of the mathematical tools suited for this problem discriminates between deterministic, and indeterministic approaches which exploit random principles to define new search directions. Evolutionary strategies [33], simulated annealing [34], and genetic algorithms [35] belong to this latter category. The present experiment uses an evolutionary strategy which processes and tunes 48 vectors of parameters for the LC voltages, starting from a random seed [36]. Adaptive step-length control [33] has been implemented to speed up the achievement of convergence.

3 Results

3.1 The one-photon Na($3s \rightarrow 3p$) *transition*

In pursuit of the goal to control the one-photon transition in sodium (see Fig. 1a) we employed phase- and amplitude shaping of the incident spectrum centered around 589 nm [37] to generate a phase-related double-pulse sequence [38]. The resulting structures were characterized by FROG [24] measurements (see Fig. 2). Moderate focusing ($f = 300$ mm) into the heat pipe resulted in a power density of $\approx 10^{11}$ W/cm^2 which was sufficient to saturate the $3s \rightarrow 3p$ transfer. The population induced in the $3p$ state was probed with a narrow-band ($\Delta\omega = 0.2$ cm^{-1}) Nd-YAG-pumped dye laser (20 μJ, 3 ns, 50 Hz) which was fired synchronous with the Ti:sapphire system and tuned to the $3p_{1/2} \rightarrow 5s$ and $3p_{3/2} \rightarrow 5s$ transitions, respectively. Pump and probe beams were aligned collinearly and diligent care was taken to ensure that the probed volume was completely overlapped by the pump.

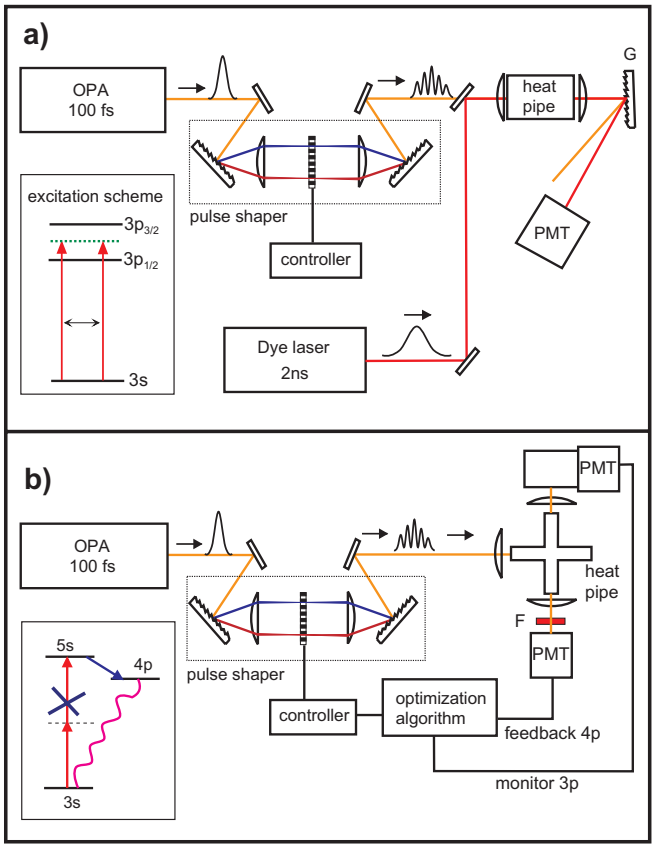

Fig. 1a,b. Experimental setup. **a** collinear pump–probe arrangement to control the one- photon excitation of Na via a double-pulse sequence. The inset illustrates the pertinent spectroscopic details. τ marks the time delay between both pulses. **b** Experimental layout and spectroscopic details of the pump- and detection schemes of the two-photon experiment. Fluorescence from $4p$ serves as feedback to the control algorithm

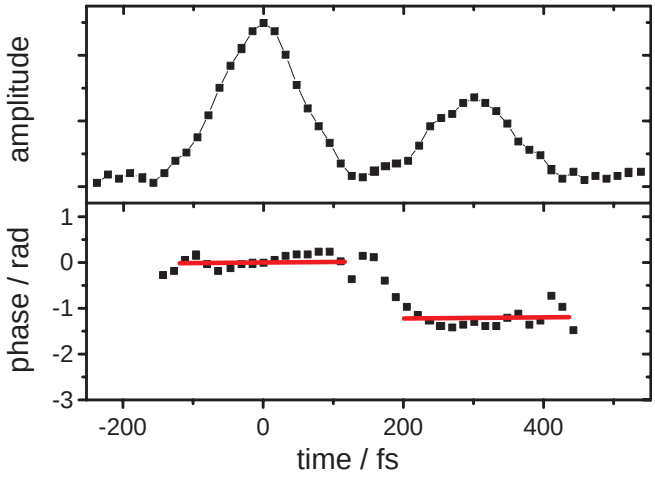

Fig. 2. Typical FROG calculation, in the time domain, of pulse envelope (*top*) and phase of a generated double pulse

In the following we will give a theoretical description of the response of this two-level system to the sequence of two phase-related pump pulses. The treatment will be restricted to the $3s(|1\rangle)$ and $3p_{1/2}(|2\rangle)$ states and the temporal evolution of the excited level as induced by the pulse pair. Coherences between the fine-split $3p$ levels due to broadband excitation are not seen as only $3p_{1/2}$ is probed. The phase of the initially excited population evolves freely in time as $\exp(\mathrm{i}\omega_{12}\,t)$ and later interferes with the different phase of the population induced by the follow-up pulse. The description of a one-photon absorption in a first-order approximation yields a population of the probed excited state which is given by $|c_2(t)|^2$, where

$$c_2\,(t) = \frac{2\pi}{\mathrm{i}h}\int_{-\infty}^{t} H_{12}^{s}\left(t'\right)\exp\left(\mathrm{i}\omega_{12}t'\right)\mathrm{d}t'\,. \tag{2}$$

$H_{12}^{s}\left(t'\right)$ is the interaction Hamiltonian which, assuming the dipole approximation, is given by $H_{12}^{s}\left(t'\right) = \mu e(t')$, where $e(t')$ symbolizes the electric field of the laser pulse. In the slowly varying envelope limit a pulse is described as a time-dependent envelope function $e(t')$ including a carrier wave with the central frequency of the laser field, ω_0. This approximation is valid for pulse durations down to a few femtoseconds. The phase of the laser pulse, $\Phi(t)$, is defined as the position of the carrier wave relative to the envelope.

A sequence of pulses with envelopes $e_n(t)$, phases $\Phi_n(t)$, and common central frequency ω_0 is described generally as:

$$E(t) = \exp(\mathrm{i}\omega_0 t)\sum_n e_n(t-t_n)\exp(i\Phi_n(t))\,. \tag{3}$$

In frequency-domain pulse shaping the tailored pulse sequence originates from a Fourier-limited incident pulse having no time-dependent phase. Hence each subpulse in (3) has its own time-independent phase and amplitude-scaled envelope of the incident pulse (Wefers and Nelson [23]). The shaping of two pulses of equal amplitude separated in time by τ is hence described by:

$$E(t) = \exp(\mathrm{i}\omega_0 t)e(t)\exp(\mathrm{i}\Phi_1) + \exp(\mathrm{i}\omega_0 t)e(t-\tau)\exp(\mathrm{i}\Phi_2)\,. \tag{4}$$

In ideal pulse shaping the phase difference $\delta\Phi = \Phi_1 - \Phi_2$ of this double-pulse pair can be chosen arbitrarily and independent of its separation in time, τ. Inserting this electric field into (2) yields a population induced in the atomic system given by [22]:

$$|c_2|^2 \propto \cos(\delta\Phi + \delta\omega\,\tau) \tag{5}$$

where $\delta\omega = \omega_{12} - \omega_0$ stands for the detuning of the laser frequency from $3s \rightarrow 3p_{1/2}$. In this model a change of the pulse-pair spacing while $\delta\Phi = \text{const.}$ induces a slow oscillation characterized by the detuning. Tuning the relative phase $\delta\Phi$ of the pulse doublet which is fixed in τ, on the other hand, again gives rise to a periodic ($1\ \mathrm{s}^{-1}$) oscillation shifted by $\delta\omega\tau$.

The experimental data presented in Fig. 3 show the population of the $3p_{1/2}$ state in dependence on an exclusive variation of either $\delta\Phi$ (Fig. 3a) or τ (Fig. 3b), respectively. While Fig. 3a agrees perfectly with Wefer's pulse-shaping model, a change of the pulse spacing seems to cause an ambiguous picture. An oscillatory behavior of the population which exceeds the capability of time resolution of our pulse-shaping setup is superimposed by a slow modulation approximately proportional to the detuning. This is in distinct contrast to the expected slow oscillation.

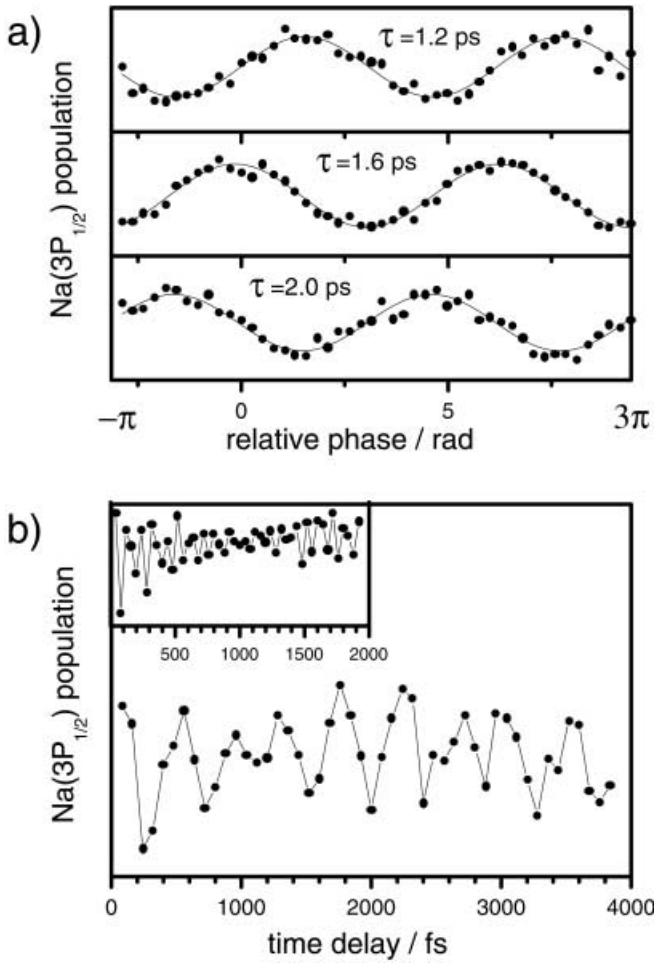

Fig. 3a,b. Population of Na($3p_{1/2}$) vs. characteristics of double pulse. **a** ϕ-transient. The relative phase is varied and plotted for three different pulse separations τ (1.2, 1.6, and 2.0 ps). **b** τ-transient. The pulses are set to equal phase while the time separation τ is changed. The resolution is 2×40 fs for the large graph and 1×40 fs for the *inset*

If the phase of each pulse could be fixed regardless of the time difference τ, as is presumed when pulse shaping is performed, only a slow oscillation should show. Referring to the experimental data we conclude that our shaper can not fix the phase of both pulses to the same value for any pulse spacing τ. As it seems, the phase of the second pulse is still dependent on its delay with respect to the first. Consequently the second pulse will induce a population with an initial phase given by this τ-dependent optical phase and the transient of τ will reproduce the superposition of the mutually independent evolutions of optical phase and free atomic phase which both depend on τ. A clear-cut discrimination of these two phase dynamics as in ideal pulse shaping, where no phase evolution of the laser field is allowed, can therefore not be expected.

Rather than resorting to pulse shaping, phase-correlated pulses may be created by interferometric superposition of two coherent beams [39, 40]. The difference in phase between the correlated pulses can not be chosen arbitrarily since they are coupled through their common carrier wave in the sense that $\delta\Phi = \omega_0\tau$. Inserting this condition into (5) leads to an altogether different dynamics in the τ-transient:

$$|c_2|^2 \propto \cos(\omega_0\tau + \delta\omega\,\tau) = \cos(\omega_{12}\tau)\,. \qquad (6)$$

A variation of the pulse-pair separation, τ, will induce rapid oscillations of the probed signal with a frequency of $\omega_{12} = 2\pi/1.97$ fs [37]. Such atomic oscillations were investigated earlier in Cs by Blanchet et al. [40].

The experimental transient reveals a beating pattern which is seemingly expressible as the sum of cosines with frequencies $\delta\omega$, ω_{12}, ω_0. Such a transient would indeed appear if, next to the two pulses of the same phase (ideal shaping, (5)), a third pulse would act upon the system which shares a common carrier wave with the pulse varied in time τ. The phases of these two pulses are coupled by $\omega_0\tau$ (6). In a detailed discussion Wefers and Nelson [23] have shown that the passively transmitting gaps of the liquid-crystal array give rise to such an additional pulse. Notwithstanding its low intensity it must be considered in the regime of saturation where this experiment was performed.

Another tentative explanation of the τ-transient rests on the assumption of a general τ-dependence of the phase of the second pulse. This would ascribe the displacement of the phase of the second pulse to inhomogeneities in our shaper.

Measurements which show the feedback of the controlled one-photon excitation to a variation of τ represent an extremely sensitive criterion of the quality of a pulse shaper incorporating a discrete mask and could serve to quantify the deviation from ideality, since an "ideal" shaper satisfies the condition formulated in (5). We propose to record the τ-transient with enhanced temporal resolution by using shorter pulses, by increasing the number of pixels, and by performing an analogous experiment addressing an atomic transition in the IR (smaller ω_{12}). This should provide us with a deeper understanding of the physical reasons which are behind these surprising results.

3.2 The two-photon Na*(3s →→ 5s) transition*

The objective of the study that will be presented in this section is the coherent control of a nonresonant two-photon process through spectral phase manipulation via feedback optimization steered by an evolutionary algorithm. A schematic diagram of the experimental layout as well as the relevant spectroscopic details of the employed pump and detection scheme are displayed in Fig. 1b. The exciting laser was tuned to $\lambda = 598$ nm which is close to the $3s \rightarrow\rightarrow 5s$ resonance, and focused to provide a maximum power density of $\approx 1 \times 10^{11}$ W/cm^2 inside the heat pipe. The population of the $5s$ target level optically decays to $3p$ or undergoes collisional relaxation to the $4p$ state. Both levels are monitored separately via their fluorescence to the $3s$ ground state at 589 nm and 330 nm, respectively.

Due to the spectral width of the ultrashort 598 nm pulses a competitive $(1+1)$-photon excitation of $5s$ via $3p$ (at 589 nm) can not be excluded rightaway. We will thus have to offer evidence that the $5s$ level is indeed populated as the result of a nonresonant two-photon absorption. In a theoretical treatment of the quantum control of multiphoton transitions by shaped ultrashort pulses which excludes strong-field effects, Meshulach et al. [41] have calculated the effect of a π phase step on the probability of N-photon absorption in a two-level system. The plots of this quantity vs. the normalized step position peak at the frequency of the N-photon absorption. They are symmetric with respect to this maximum and

vanish for N values of the phase step position. The number of minima is thus indicative of the order of the absorption process.

Figure 4 shows our experimental result for the $3s \rightarrow\rightarrow 5s$ transition as a function of the step position induced by the SLM. The position of the maximum and the occurrence of two symmetrically arranged minima suggest a two-photon process induced by a wavelength of ≈ 602 nm. This number is directly read from a spectrum of the laser pulse which was taken while pixel #43 (maximum) was blocked (see Fig. 4).

The implementation of a feedback-controlled optimization routine requires to identify an observable which is uniquely tied to the quantity to be controlled. Population of $5s$ gives rise to fluorescence from the $3p$ and $4p$ levels. $3p$ may, however, also be pumped in a 589 nm one-photon step from $3s$. The text to follow describes two experiments which address and settle this tentativeness.

The data of the first test are illustrated in Fig. 5 and show the fluorescence from the $3p$ and $4p$ levels, following excitation of $5s$ by 1 mW of unchanged or modified pump pulses. The latter were obtained by clipping, in the Fourier plane, the blue wings (< 591 nm) of the frequency spectrum. The ensuing pulse spectrum is shown in the right panel of Fig. 4. Fluorescence from $4p$ appears with equal intensity for either excitation condition. The $3p$ analog, however, is drastically diminished in the absence of the wavelength matching the one-photon resonance.

The previous measurement strongly indicates that $5s$, which is the precursor to $4p$, is accessed nonresonantly, rather than by a $(1+1)$-sequence. Supporting evidence comes from an examination of the fluorescence intensities vs. laser power, which is displayed in Fig. 6. Again, the $4p$ signal appears unimpressed by the particularities of the pump laser's frequency profile and exhibits a quadratic slope, indicative of a two-photon process. The $3p$ data are more complex. In the presence of 589 nm the signal behaves linearly for low laser intensity and scales $\propto I^{3/2}$ above approximately 0.2 mW, pointing to saturation [42]. Blocking the resonant wavelength produces the same low-intensity behavior, but a quadratic slope beyond 0.2 mW.

The bottom line of the conclusions which may be drawn from both checks is as follows: given the conditions of our experiment (pump ≈ 1 mW), $4p$ is exclusively fed from $5s$ which owes its population to a nonresonant two-photon excitation. The $3p$ state draws to some extent from $5s$, but is predominantly pumped in a resonant single step when the pulse is left unmodified. We may thus apply Meshulach's model [41] to describe the coherently controlled population of Na($5s$) and we have identified $4p$ fluorescence as a directly linked criterion which is suited to serve as input to the steering algorithm which updates the modulator.

The nonresonant two-photon interaction of an ultrashort pulse with a two-level system induces a transition with

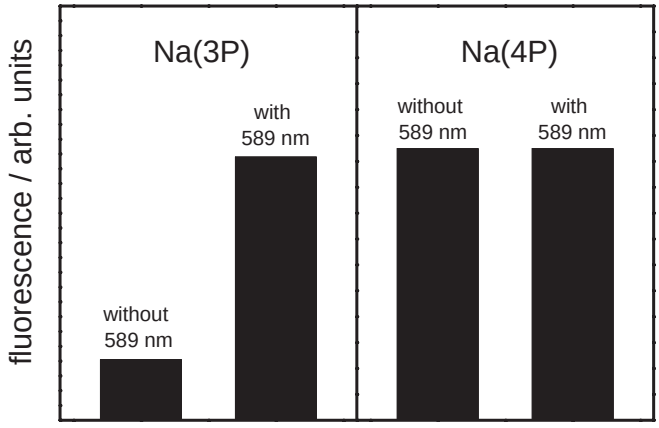

Fig. 5. Response of $3p$ and $4p$ fluorescence to the presence or absence of 589 nm light (one-photon resonance)

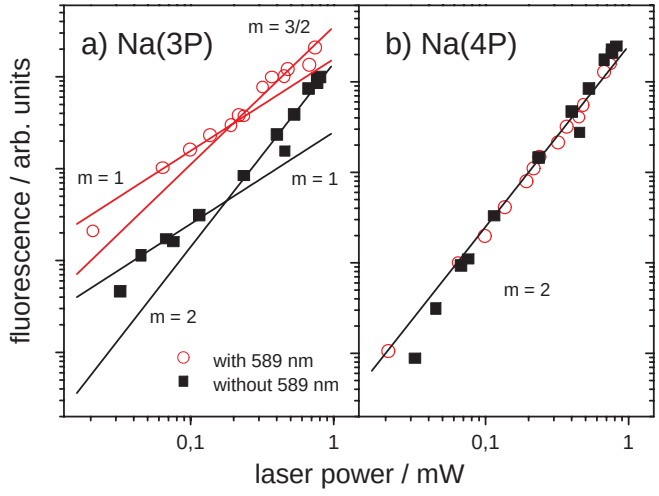

Fig. 6. Power dependence of $3p$ and $4p$ fluorescence with or without 589 nm light

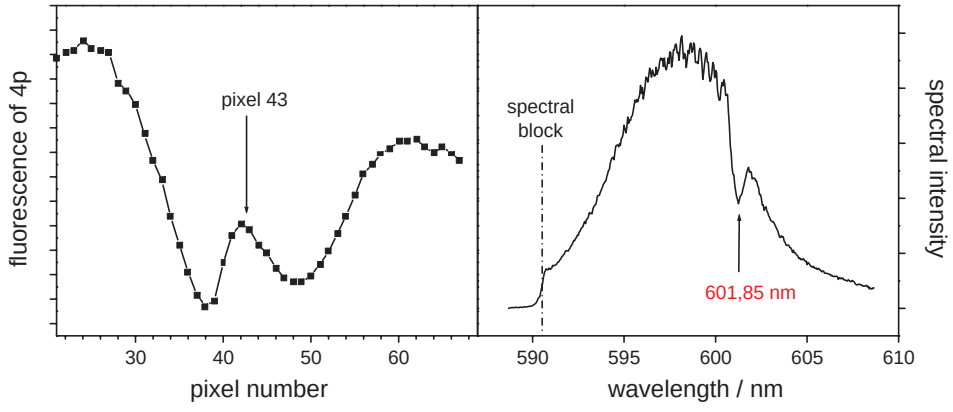

Fig. 4. *Left*: phase step shifted across the mask. Fluorescence from collisionally populated $4p$ shows symmetry around pixel #43. *Right*: OPA spectrum behind SLM observed with pixel #43 shut and left wing clipped by blocking part of spectrum

a probability S_2 [43]:

$$S_2 = \left| \int A\left(\frac{\omega_0}{2}+\Omega\right) A\left(\frac{\omega_0}{2}-\Omega\right) \times \exp\left\{ \mathrm{i} \underbrace{\left[\Phi\left(\frac{\omega_0}{2}+\Omega\right) + \Phi\left(\frac{\omega_0}{2}-\Omega\right) \right]}_{\text{interference term}} \right\} \mathrm{d}\Omega \right|^2 \qquad (7)$$

where ω_0 is the energy of the $3s \rightarrow 5s$ transition which corresponds to 301 nm [37]. Two-photon transitions occur for all pairs of photons which satisfy the condition $\omega_1 + \omega_2 = \omega_0$. The detuning of frequencies ω_1, ω_2 from $\omega_0/2$ is denoted by Ω. Control of the excitation process is exercised via the interference term and can either maximize or minimize the probability S_2, as Meshulach et al. [41, 43] have recently demonstrated for the nonresonant two-photon transition of caesium. Maximization is obviously achieved if the interference term vanishes, which describes the minimum-duration transform-limited pulse. This solution is not singular, however, since any shaped pulse with the same power spectrum $A(\omega)$ but with an antisymmetric phase function, $\Phi(\omega_0/2-\Omega) = -\Phi(\omega_0/2+\Omega)$, will yield the same result, irrespective of the particular appearance of the phase distribution. This result is counterintuitive since longer, i.e. less-intense, pulses should be less effective in transferring population. In their paper, Meshulach et al. [43] have also formulated phase requirements to produce so-called *dark pulses* which altogether cancel the two-photon pumping probability. No net transitions are induced as long as $\Phi(\Omega) = \cos(\beta\Omega)$.The total of solutions, discriminated by virtue of the parameter β, is symmetric with respect to the center frequency $\omega_0/2$.

In the present experiment the designed pulses were created by phase-only modulation [38]. The task to pinpoint the conditions which either maximize or cancel S_2 was left to an evolutionary strategy which was integrated in a feedback loop. Unbiased by any a-priori modeling the algorithm set out from a phase filter $\Phi(n) = a\cos(bn+c)$ with n as the variable which numbers the LC pixels, and a, b, and c as free parameters to be optimized. This approach is still tractable but sufficiently general to comprise Meshulach's solution [43]. The experiment was run repeatedly for either objective and achieved convergence within five generations. The phase filters which were retrieved as a result of the optimization procedure are symmetric (cosine) in the case of extinction, and antisymmetric (sine) in the case of enhancement of fluorescence. Symmetry persists with reference to the center frequency $\omega_0/2$ which impinges on strip #43 (see Fig. 7). This good agreement with theory which this three-parameter optimization produces requires to impose upper and lower restrictions on the parameter b. In the bright-pulse case b must be sufficiently large to allow at least four oscillations of the phase over the width of the mask. In the absence of this lower limit the algorithm would merely compensate the chirp of the incoming pulse to produce the Fourier-limited shape, i.e. the pulse having the minimum time duration, which obviously maximizes S_2. To optimize the dark pulses b has been limited to yield a maximum of eight phase oscillations. Lifting this restriction would result in very long pulses which are dark due to insufficient intensity.

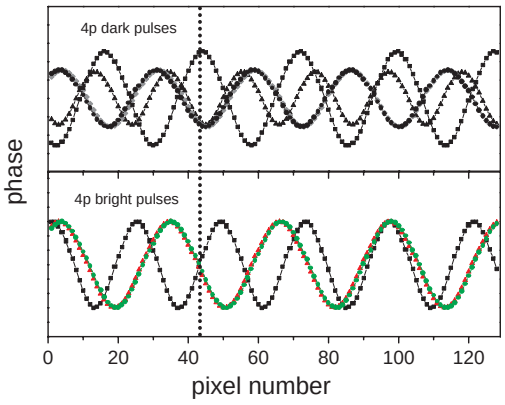

Fig. 7. Periodic phase functions obtained from three (*top*) and two consecutive optimization runs. In accordance with theory, traces show symmetry for dark and antisymmetry for bright pulses. *Dotted line* marks pixel #43

In a further experiment we lifted the restriction on the dimensionality of the parameter space and tried a model of the phase filter which permitted an unbiased choice of parameters. Aiming at the generation of dark pulses we introduced a phase function defined by the minimum number of sampling points connected by a linear interpolation. Each of these points may assume 64 discrete values within a range from 0 to 2π. Six parameters proved sufficient to achieve this goal. The dark pulse retrieved by the algorithm is shown in Fig. 8a whereas Fig. 8b represents the phase setting of the mask. The property of being "dark" is indeed phase-related, which is convincingly shown by comparison with the effect induced by a chirped pulse of equivalent energy and duration. The evolution of a dark pulse as mirrored by the decrease of the $4p$ fluorescence feedback signal is shown in the right column of Fig. 9. Compared to an unmodulated pulse the $5s$ population is reduced to $< 3\%$. The left panel proves the insensitivity of the one-photon $3s \rightarrow 3p$ transition to a phase-only modulation. Once the resonant pumping of $3p$ is suppressed by blocking the relevant wavelength the fluorescence from this level perfectly matches that of $4p$ (Fig. 9, bottom row). $3p$ is now populated via radiative decay of $5s$ and is hence equally suited as feedback input.

Both, the three- as well as the six-parameter approach converge after less than 10 generations, i.e. within less than five minutes. A comparative inspection of the phase functions returned by either method raised the question of the existence of additional solutions which are of altogether different character. We thus expanded the previous parametrization

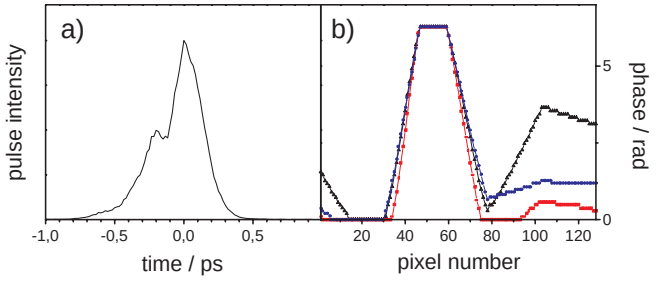

Fig. 8a,b. Free optimization using a six-parameter phase function with linear interpolation. **a** Cross-correlation of a typical dark pulse. **b** Phase values as achieved in three different runs

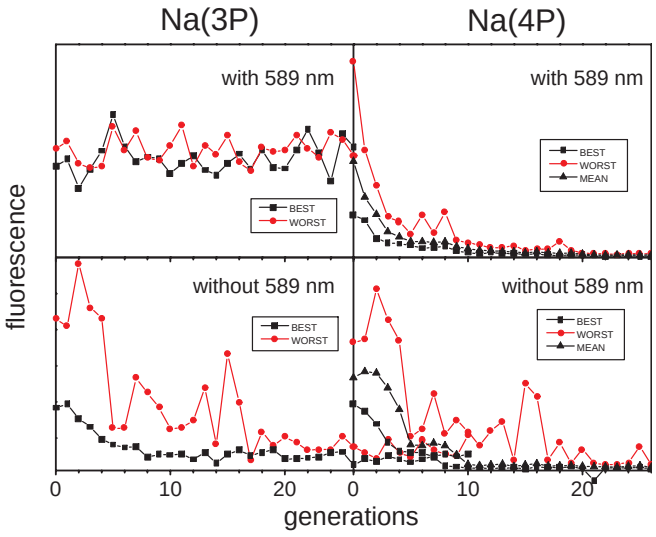

Fig. 9. Convergence data of the six-parameter search for the dark pulse. Figure shows the best and worst mask patterns for each generation. As long as 589 nm light is blocked, $3p$ and $4p$ fluorescence are equally suited as feedback signal. This is not the case if one-photon transitions are admitted since the direct excitation of $3p$ is phase insensitive

to 128 sample points, each falling between 0 and 2π as before. Figure 10 documents the convergence towards the dark (left) and the bright pulse (right) which was attained after ≈ 10 generations. In accordance with theory an antisymmetric phase function causes population enhancement (Fig. 10b). No likewise apparent symmetry properties, however, characterize the suppression of two-photon pumping. Re-runs of the optimization procedure produced identical experimental results but differing phase functions. The solutions which the algorithm produced bore no resemblance with the prediction of theory. The shaped pulses show a complex phase- and amplitude-time structure of comparable duration (≈ 2 ps). It is thus not their peak power but rather their phase distribution which produces qualities such as "bright" or "dark".

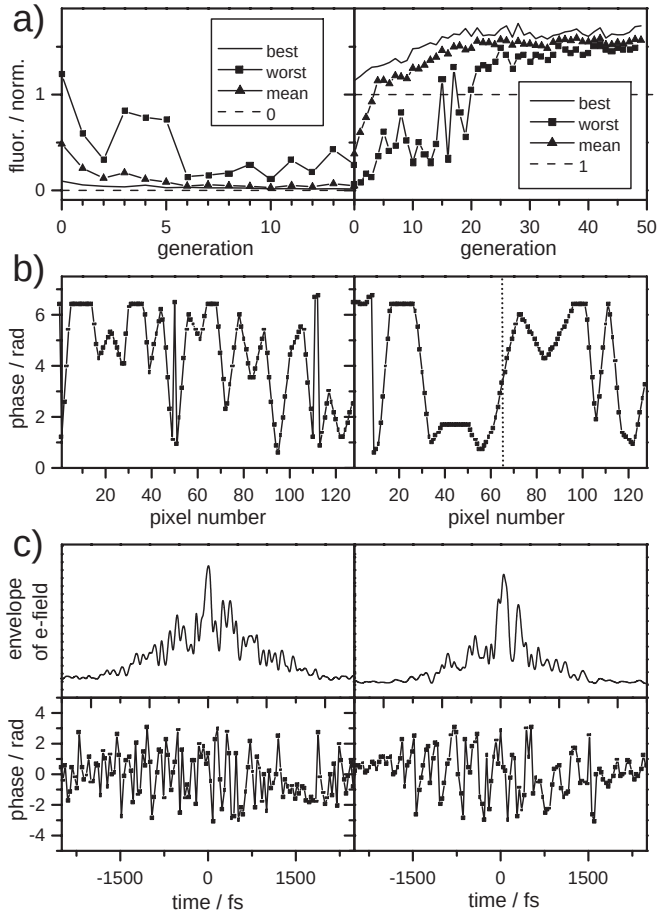

Fig. 10a–c. Convergence data of the 128-parameter search for the dark (*left*) and bright (*right*) pulse. **a** Normalized fluorescence intensity to document convergence. *Dashed lines* mark "no signal" (0) and "unshaped reference pulse" (1). **b** *Right*: phase structure of bright pulse showing antisymmetry. Reference position has shifted to pixel 64 ($\widehat{=}$ 602 nm) due to re-alignment of optical setup. **c** Pulse shape and phase structure in the time domain. *Bright* and *dark pulses* show a complex structure, but note their similar durations

4 Conclusion

In this paper we studied the influence of phase-modulated fs laser pulses on one- and two-photon transitions in an atomic prototype system and tested the implementation of a feedback loop using evolutionary algorithms.

The one-photon transition presents an excellent tool to test the quality of phase-related pulses, as the excitation of the $3p$ level in sodium depends critically on the relative phase of the double pulse. It has been shown that the experimental outcome could be explained by a combination of two limiting cases. The relative contribution depends on the nature of the phase coupling within the pulse sequence, which is influenced by the experimental conditions of the setup.

The phase-modulated excitation of the two-photon transition shows that the feedback approach can be successfully used to find fs laser pulses for different control objectives, even without an intelligent initial guess supplied by theory. The best solutions for both extremes were obtained within five generations. By allowing the feedback algorithm to search in an extended parameter space the algorithm found new phase structures in addition to known analytic solutions. These structures are not intuitively understandable and call for further theoretical studies.

Since the approach of feedback optimization using evolutionary algorithms works well in an atomic prototype system the path ahead is now open to find optical pulses for different objectives in even more complex systems without prior knowledge of the spectroscopic details [1–3]. As an example, it should now be possible to find laser pulses which give rise to light-induced transparency, as well as lasers without inversion, even for complex multi-level systems. The feedback approach also offers the possibility to suppress unwanted competitive multiphoton absorptions while a specific transition is excited with high intensity. This might be important when the collision complex of a chemical reaction is investigated with broadband fs laser pulses in real time via photoassociation processes, where the excitation of the complex occurs near a one-photon resonance and high intensities are necessary.

Acknowledgements. The authors thank T. Lang and H. Bauer for their technical assistance. Financial support by the DFG-Schwerpunkt "Femtosekunden-Spektroskopie" is gratefully acknowledged.

References

1. C.J. Bardeen, V.V. Yakovlev, K.R. Wilson, S.D. Carpenter, P.M. Weber, W.S. Warren: Chem. Phys. Lett. **280**, 151 (1997)
2. A. Assion, T. Baumert, M. Bergt, T. Brixner, B. Kiefer, V. Seyfried, M. Strehle, G. Gerber: Science **282**, 919 (1998)
3. T.C. Weinacht, J. Ahn, P.H. Bucksbaum: Nature **397**, 233 (1999)
4. P. Gaspard, I. Burghardt (Eds.): *Chemical Reactions and their Control on the Femtosecond Time Scale*, Vol. 101 (Wiley, New York 1997)
5. S.A. Rice: Science **258**, 412 (1992)
6. P. Brumer, M. Shapiro: Sci. Am. **272**, 34 (1995)
7. W.S. Warren, H. Rabitz, M. Dahleh: Science **259**, 1581 (1993)
8. A.M. Weiner, J.P. Heritage, E.M. Kirschner: J. Opt. Soc. Am., B: Opt. Phys. **5**, 1563 (1988)
9. A.M. Weiner, D.E. Leaird, J.S. Patel, J.R. Wullert: Opt. Lett. **15**, 326 (1990)
10. A.M. Weiner, D.E. Leaird, J.S. Patel, J.R. Wullert: IEEE J. Quantum Electron. **QE-28**, 908 (1992)
11. A.M. Weiner: Prog. Quantum Electron. **19**, 161 (1995)
12. M.M. Wefers, K.A. Nelson: Opt. Lett. **18**, 2032 (1993)
13. M.M. Wefers, K.A. Nelson: Opt. Lett. **20**, 1047 (1995)
14. J.X. Tull, M.A. Dugan, W.S. Warren: Adv. Magn. Opt. Reson. **20**, 1 (1997)
15. C. Dorrer, F. Salin, F. Verluise, J.P. Huignard: Opt. Lett. **23**, 709 (1998)
16. E. Zeek, K. Maginnis, S. Backus, R. Russek, M. Murnane, G. Mourou, H. Kapteyn: Opt. Lett. **24**, 493 (1999)
17. R.S. Judson, H. Rabitz: Phys. Rev. Lett. **68**, 1500 (1992)
18. D. Meshulach, D. Yelin, Y. Silberberg: Opt. Commun. **138**, 345 (1997)
19. D. Meshulach, D. Yelin, Y. Silberberg: J. Opt. Soc. Am., B: Opt. Phys. **15**, 1615 (1998)
20. T. Baumert, T. Brixner, V. Seyfried, M. Strehle, G. Gerber: Appl. Phys. B **65**, 779 (1997)
21. D. Zeidler, T. Hornung, D. Proch, M. Motzkus: Appl. Phys. B **70**[Suppl.], S125–S131 (2000)
22. M.M. Wefers, H. Kawashima, K.A. Nelson: J. Chem. Phys. **102**, 9133 (1995)
23. M.M. Wefers, K.A. Nelson: J. Opt. Soc. Am., B: Opt. Phys. **12**, 1343 (1995)
24. R. Trebino, K.W. DeLong, D.N. Fittinghoff, J.N. Sweetser, M.A. Krumbügel, B.A. Richman, D.J. Kane: Rev. Sci. Instrum. **68**, 3277 (1997)
25. C.R. Vidal: In *Atomic, Molecular, and Optical Physics: Atoms and Molecules*, Vol. 29B, ed. by F.B. Dunning, R.G. Hulet (Academic Press, San Diego 1996) p. 67
26. M.D. Crisp: Phys. Rev., A **1**, 1604 (1970)
27. J.K. Ranka, R.W. Schirmer, A.L. Gaeta: Phys. Rev. A **57**, R36 (1998)
28. M.M. Wefers, K.A. Nelson: IEEE J. Quantum Electron. **QE-32**, 161 (1996)
29. T. Hornung: Diplomarbeit (internal report MPQ 247) (Technische Universität München 1999)
30. A.M. Weiner, S. Oudin, D.E. Leaird, D.H. Reitze: J. Opt. Soc. Am., A: Opt. Im. Sci. **10**, 1112 (1993)
31. K. Takasago, T. Itoh, M. Takekawa, K.-I. Utoh, F. Kannari: Jpn. J. Appl. Phys. **35**, 624 (1996)
32. K. Takasago, M. Takekawa, M. Suzuki, K. Komori, F. Kannari: IEEE J. Quantum Electron. **QE-4**, 346 (1998)
33. H.P. Schwefel: *Evolution and Optimum Seeking* (Wiley, New York 1995)
34. B. Amstrup, J.D. Doll, R.A. Sauerbrey, G. Szabó, A. Lörincz: Phys. Rev. A **48**, 3830 (1993)
35. D.E. Goldberg: *Genetic Algorithms in Search, Optimization, and Machine Learning* (Addison-Wesley, Reading 1993)
36. D. Zeidler, T. Hornung, M. Motzkus: paper Q 36.4, presented at Frühjahrstagung der DPG (Heidelberg 1999)
37. A. Lindgård, S.E. Nielsen: At. Data Nucl. Data Tab. **19**, 571 (1977)
38. T. Hornung, D. Zeidler, K.-L. Kompa, M. Motzkus: paper Q 4.5, presented at Frühjahrstagung der DPG (Heidelberg 1999)
39. N.F. Scherer, A. Matro, L.D. Ziegler, M. Du, R.J. Carlson, J.A. Cina, G.R. Fleming: J. Chem. Phys. **96**, 4180 (1992)
40. V. Blanchet, M.A. Bouchene, B. Girard: J. Chem. Phys. **108**, 4862 (1998)
41. D. Meshulach, Y. Silberberg: Phys. Rev. A **60**, 1287 (1999)
42. S. Speiser, J. Jortner: Chem. Phys. Lett. **44**, 399 (1976)
43. D. Meshulach, Y. Silberberg: Nature (London) **396**, 239 (1998)